Scalable Adaptive Multitarget Tracking Using Multiple Sensors

Florian Meyer*, Paolo Braca*, Franz Hlawatsch†, Michele Micheli*, and Kevin D. LePage*

*Centre for Maritime Research and Experimentation, La Spezia, Italy (firstname.lastname@cmre.nato.int)
†Institute of Telecommunications, TU Wien, Vienna, Austria (franz.hlawatsch@tuwien.ac.at)

***Abstract*—In networked mobile multitarget tracking systems, parameters such as detection probabilities, clutter rates, and motion model parameters are often unknown and time-varying. Such parameter variability can seriously degrade the performance of a multitarget tracking system. Here, we propose a Bayesian tracking framework in which the multisensor-multitarget tracking problem is formulated according to the measurement origin uncertainty paradigm and the unknown parameters—in the present case, the detection probabilities at the individual sensors—are modeled as Markov chains. The resulting Bayesian estimation problem is then solved using the belief propagation scheme. This approach results in a multisensor-multitarget tracking method that is able to adapt to the time variations of the detection probabilities. Moreover, the method has a low complexity that scales very well in all relevant system parameters. The performance of the method is assessed using data collected by a mobile underwater wireless sensor network.**

***Index Terms*—Multitarget tracking, data association, belief propagation, message passing, factor graph, adaptive algorithm, underwater sensor network.**

I. Introduction

Multitarget tracking is important in many applications including air traffic control, biomedical analytics, robotics, oceanography, and surveillance. A difficulty in most applications is the fact that the number of targets and the association between measurements and targets are unknown [1], [2]. Furthermore, in the case of low-observable targets, i.e., targets leading to measurements with a low signal-to-noise ratio, multiple sensors are required. However, most multisensor methods for multitarget tracking [2]–[8] either perform approximations of unknown fidelity and thus may not be able to fully realize the performance gains offered by multiple sensors, or they scale poorly in relevant system parameters. In [9], we proposed a multisensor-multitarget tracking method based on the belief propagation (BP) scheme. This method allows for an unknown number of targets up to a predefined maximum number. In contrast to random finite set based techniques [2], [6]–[8], the joint target state is ordered and has a fixed number of components. The method combines good performance with an attractive scaling of computational complexity, which is quadratic in the number of targets and linear in the number of sensors and in the number of measurements per sensors.

Almost all multitarget tracking methods (exceptions include [10]–[12]) assume fixed and known "environmental parameters" such as probability of detection at the sensors, clutter intensity profile, and target motion parameters. In practice, however, these parameters are typically unknown and time-varying [10]–[12]. In particular, the probabilities of observing (detecting) a target by the sensors often depend on unknown factors such as the aspect—e.g., radar cross section—of the target or certain characteristics of the environment.

Here, we address this issue by proposing an extension of our BP-based multisensor-multitarget tracking method [9] to unknown and time-varying probabilities of detection at the sensors. In the proposed method, these detection probabilities are tracked along with the target states. In this way, our method is able to adapt to changes in the detection probabilities while retaining the excellent scaling properties of the original method [9]. We note that our adaptive approach can be easily used also for other unknown and time-varying parameters, such as the clutter intensity profile and target motion parameters. We present results of an underwater acoustic tracking experiment and show that our adaptive method can outperform the original nonadaptive method using manually tuned detection probabilities.

This paper is organized as follows. In Section II, we describe the system model and a corresponding statistical formulation. In Section III, we develop the proposed method. Finally, the performance of the method in a multistatic sonar tracking experiment is evaluated in Section IV.

II. System Model and Statistical Formulation

The system model and basic statistical formulation underlying our method are as in [9, Sec. II], except for an explicit modeling of random detection probabilities.

A. Targets, Sensors, Measurements

There are K *potential targets* $k \in \mathcal{K} \triangleq \{1, \ldots, K\}$. The existence of potential target k at time n is indicated by $r_{n,k} \in \{0, 1\}$, i.e., target k exists at time n if $r_{n,k} = 1$. The state $\mathbf{x}_{n,k}$ of target k at time n consists of the target's position and possibly further parameters. For mathematical convenience, the state $\mathbf{x}_{n,k}$ also exists (formally) for a nonexistent target k. We define the *augmented state* $\mathbf{y}_{n,k} \triangleq [\mathbf{x}_{n,k}^{\mathrm{T}} \; r_{n,k}]^{\mathrm{T}}$ and the vectors $\mathbf{y}_n \triangleq \left[\mathbf{y}_{n,1}^{\mathrm{T}} \cdots \mathbf{y}_{n,K}^{\mathrm{T}}\right]^{\mathrm{T}}$ and $\mathbf{r}_n \triangleq \left[r_{n,1} \cdots r_{n,K}\right]^{\mathrm{T}}$.

There are S sensors $s \in \mathcal{S} \triangleq \{1, \ldots, S\}$. At time n, sensor s generates $M_n^{(s)}$ measurements $\mathbf{z}_{n,m}^{(s)}$, $m \in \mathcal{M}_n^{(s)} \triangleq \{1, \ldots, M_n^{(s)}\}$ via a detection process. We define $\mathbf{z}_n^{(s)} \triangleq \left[\mathbf{z}_{n,1}^{(s)\mathrm{T}} \cdots \mathbf{z}_{n,M_n^{(s)}}^{(s)\mathrm{T}}\right]^{\mathrm{T}}$, $\mathbf{z}_n \triangleq \left[\mathbf{z}_n^{(1)\mathrm{T}} \cdots \mathbf{z}_n^{(S)\mathrm{T}}\right]^{\mathrm{T}}$, and $\mathbf{m}_n \triangleq \left[M_n^{(1)} \cdots\right.$

$M_n^{(S)}\big]^{\mathrm{T}}$. There is a data association (measurement origin) uncertainty: it is not known which measurement $\mathbf{z}_{n,m}^{(s)}$ was generated by which target k, and it is possible that $\mathbf{z}_{n,m}^{(s)}$ was not generated by any target (false alarm, clutter) or that a target did not generate any measurement of sensor s (missed detection) [1], [2]. Assuming that a target can generate at most one measurement at sensor s and a measurement at sensor s can be generated by at most one target [1], [2], the measurement-target associations at sensor s are described by the vector $\mathbf{a}_n^{(s)} = \big[a_{n,1}^{(s)} \cdots a_{n,K}^{(s)}\big]^{\mathrm{T}}$ with entries

$$a_{n,k}^{(s)} \triangleq \begin{cases} m \in \mathcal{M}_n^{(s)}, & \text{if at time } n, \text{ potential target } k \text{ generates measurement } m \text{ at sensor } s \\ 0, & \text{if at time } n, \text{ potential target } k \text{ is not detected by sensor } s. \end{cases}$$

Alternatively, the measurement-target associations can be described by the vector $\mathbf{b}_n^{(s)} = \big[b_{n,1}^{(s)} \cdots b_{n,M_n^{(s)}}^{(s)}\big]^{\mathrm{T}}$ with entries

$$b_{n,m}^{(s)} \triangleq \begin{cases} k \in \mathcal{K}, & \text{if at time } n, \text{ measurement } m \text{ at sensor } s \text{ is generated by potential target } k \\ 0, & \text{if at time } n, \text{ measurement } m \text{ at sensor } s \text{ is not generated by a potential target.} \end{cases}$$

We also define $\mathbf{a}_n \triangleq \big[\mathbf{a}_n^{(1)\mathrm{T}} \cdots \mathbf{a}_n^{(S)\mathrm{T}}\big]^{\mathrm{T}}$ and $\mathbf{b}_n \triangleq \big[\mathbf{b}_n^{(1)\mathrm{T}} \cdots \mathbf{b}_n^{(S)\mathrm{T}}\big]^{\mathrm{T}}$. Note that $\mathbf{b}_n$ can be derived from $\mathbf{a}_n$ and vice versa. Following [9], [13], this redundant formulation of data association uncertainty is an important basis of our method.

B. Target Statistics

Let $\phi(\mathbf{y}_{n,k}) = \phi(\mathbf{x}_{n,k}, r_{n,k})$ denote generically a probability density function (pdf) or BP message defined for an augmented state $\mathbf{y}_{n,k} = [\mathbf{x}_{n,k}^{\mathrm{T}}\ r_{n,k}]^{\mathrm{T}}$. The state $\mathbf{x}_{n,k}$ of a nonexisting target k (i.e., with $r_{n,k} = 0$) is formally defined but obviously irrelevant. Therefore, we set $\phi(\mathbf{x}_{n,k}, 0) = \phi_{n,k}\, f_{\mathrm{D}}(\mathbf{x}_{n,k})$, where $f_{\mathrm{D}}(\mathbf{x}_{n,k})$ is a "dummy pdf." As shown in [9], $f_{\mathrm{D}}(\mathbf{x}_{n,k})$ must be 1 on an arbitrary support of area/volume 1 and 0 outside that support, which implies the property $f_{\mathrm{D}}^2(\mathbf{x}_{n,k}) = f_{\mathrm{D}}(\mathbf{x}_{n,k})$. Let $\phi(r_{n,k}) \triangleq \int \phi(\mathbf{x}_{n,k}, r_{n,k})\, \mathrm{d}\mathbf{x}_{n,k}$, and note that $\phi(0) = \phi_{n,k}$. If $\phi(\mathbf{x}_{n,k}, r_{n,k})$ is normalized, i.e.,

$$\sum_{r_{n,k} \in \{0,1\}} \int \phi(\mathbf{x}_{n,k}, r_{n,k})\, \mathrm{d}\mathbf{x}_{n,k} = \phi(0) + \phi(1) = 1,$$

then one can interpret $\phi(0) = \phi_{n,k}$ as the probability that potential target k does not exist and $\phi(1)$ as the probability that potential target k exists.

If potential target k did not exist at time $n-1$, i.e., $r_{n-1,k} = 0$, then the probability that it exists at time n, i.e., $r_{n,k} = 1$, is given by the birth probability $p_{n,k}^{\mathrm{b}}$, and if it does exist at time n, its state $\mathbf{x}_{n,k}$ is distributed according to the birth pdf $f_{\mathrm{b}}(\mathbf{x}_{n,k})$. If potential target k existed at time $n-1$, i.e., $r_{n-1,k} = 1$, then the probability that it still exists at time n, i.e., $r_{n,k} = 1$, is given by the survival probability $p_{n,k}^{\mathrm{s}}$, and if it still exists at time n, its state $\mathbf{x}_{n,k}$ is distributed according to the state transition pdf $f(\mathbf{x}_{n,k}|\mathbf{x}_{n-1,k})$. For $n \geq 0$, the augmented target states $\mathbf{y}_{n,k}$ are assumed to evolve independently according to Markovian dynamic models [1], [2], and at time $n = 0$, they are assumed statistically independent (across k) with prior pdfs $f(\mathbf{y}_{0,k}) = f(\mathbf{x}_{0,k}, r_{0,k})$. It follows that the pdf of $\mathbf{y} \triangleq \big[\mathbf{y}_0^{\mathrm{T}} \cdots \mathbf{y}_n^{\mathrm{T}}\big]^{\mathrm{T}}$ factorizes as

$$f(\mathbf{y}) = \prod_{k=1}^{K} f(\mathbf{y}_{0,k}) \prod_{n'=1}^{n} f(\mathbf{y}_{n',k}|\mathbf{y}_{n'-1,k}). \tag{1}$$

An expression of $f(\mathbf{y}_{n,k}|\mathbf{y}_{n-1,k}) = f(\mathbf{x}_{n,k}, r_{n,k}|\mathbf{x}_{n-1,k}, r_{n-1,k})$ in terms of $p_{n,k}^{\mathrm{b}}$, $f_{\mathrm{b}}(\mathbf{x}_{n,k})$, $p_{n,k}^{\mathrm{s}}$, and $f(\mathbf{x}_{n,k}|\mathbf{x}_{n-1,k})$ is provided in [9].

C. Likelihood Function

The distribution of measurement $\mathbf{z}_{n,m}^{(s)}$ is described by the pdf $f\big(\mathbf{z}_{n,m}^{(s)}\big|\mathbf{x}_{n,k}\big)$ if $\mathbf{z}_{n,m}^{(s)}$ is generated by target k (i.e., $a_{n,k}^{(s)} = m \in \mathcal{M}_n^{(s)}$), and by $f_{\mathrm{FA}}\big(\mathbf{z}_{n,m}^{(s)}\big)$ if $\mathbf{z}_{n,m}^{(s)}$ is a false alarm (i.e., $a_{n,k}^{(s)} = 0$). The number of false alarms is assumed Poisson distributed with mean $\mu^{(s)}$. Let $\mathbf{z} \triangleq \big[\mathbf{z}_1^{\mathrm{T}} \cdots \mathbf{z}_n^{\mathrm{T}}\big]^{\mathrm{T}}$, $\mathbf{a} \triangleq \big[\mathbf{a}_1^{\mathrm{T}} \cdots \mathbf{a}_n^{\mathrm{T}}\big]^{\mathrm{T}}$, and $\mathbf{m} \triangleq \big[\mathbf{m}_1^{\mathrm{T}} \cdots \mathbf{m}_n^{\mathrm{T}}\big]^{\mathrm{T}}$. Under commonly used assumptions, the "total likelihood function" $f(\mathbf{z}|\mathbf{y}, \mathbf{a}, \mathbf{m})$ is obtained as [1], [2], [9]

$$f(\mathbf{z}|\mathbf{y}, \mathbf{a}, \mathbf{m}) = C(\mathbf{z}) \prod_{n'=1}^{n} \prod_{s=1}^{S} \prod_{k=1}^{K} g\big(\mathbf{x}_{n',k}, r_{n',k}, a_{n',k}^{(s)}; \mathbf{z}_{n'}^{(s)}\big), \tag{2}$$

where $C(\mathbf{z})$ is a normalization factor and $g\big(\mathbf{x}_{n,k}, r_{n,k}, a_{n,k}^{(s)}; \mathbf{z}_n^{(s)}\big)$ is given by

$$g\big(\mathbf{x}_{n,k}, 1, a_{n,k}^{(s)}; \mathbf{z}_n^{(s)}\big) = \begin{cases} \dfrac{f\big(\mathbf{z}_{n,m}^{(s)}\big|\mathbf{x}_{n,k}\big)}{f_{\mathrm{FA}}\big(\mathbf{z}_{n,m}^{(s)}\big)}, & a_{n,k}^{(s)} = m \in \mathcal{M}_n^{(s)} \\ 1, & a_{n,k}^{(s)} = 0 \end{cases}$$

$$g\big(\mathbf{x}_{n,k}, 0, a_{n,k}^{(s)}; \mathbf{z}_n^{(s)}\big) = 1.$$

D. Probability of Detection

An existing target k is detected by sensor s with an unknown, time-varying probability $q_{n,k}^{(s)}$. We define $\mathbf{q}$ to be the vector of all $q_{n',k}^{(s)}$ for n' up to time n. Differently from our previous work in [9], and following [12], we model the $q_{n,k}^{(s)}$ as random variables that take their values from a finite set $\mathcal{Q} = \{\omega_1, \ldots, \omega_Q\}$, where $\omega_i \in (0, 1]$. We assume that the $q_{n,k}^{(s)}$ are independent across k and s and independent of $\mathbf{y}$. The temporal evolution of $q_{n,k}^{(s)}$ is modeled by a Markov chain with a transition matrix $\mathbf{Q}^{(s)} \in (0, 1]^{Q \times Q}$ that is equal for all targets k. Thus, the transition probability of $q_{n,k}^{(s)}$ is given by $p\big(q_{n,k}^{(s)} = \omega_j \big| q_{n-1,k}^{(s)} = \omega_i\big) = \big[\mathbf{Q}^{(s)}\big]_{i,j}$. Note that $\sum_{j=1}^{Q} \big[\mathbf{Q}^{(s)}\big]_{i,j} = 1$ for all $i \in \{1, \ldots, Q\}$. The initial distribution of $q_{n,k}^{(s)}$ is given by the probability mass function (pmf) $p\big(q_{0,k}^{(s)}\big)$. It follows that the prior pmf of $\mathbf{q}$ factorizes as

$$p(\mathbf{q}) = \prod_{s=1}^{S} \prod_{k=1}^{K} p\big(q_{0,k}^{(s)}\big) \prod_{n'=1}^{n} p\big(q_{n',k}^{(s)} \big| q_{n'-1,k}^{(s)}\big). \tag{3}$$

E. Joint Prior Distribution of Association Variables and Numbers of Measurements

Let $1(a)$ denote the indicator function of the event $a=0$, i.e., $1(a)$ equals 1 if $a=0$ and 0 otherwise. Under commonly used assumptions, the joint prior pmf of $\mathbf{a}$, $\mathbf{b} \triangleq \big[\mathbf{b}_1^{\mathrm{T}} \cdots \mathbf{b}_n^{\mathrm{T}}\big]^{\mathrm{T}}$, and $\mathbf{m}$ given $\mathbf{y}$ and $\mathbf{q}$ can be expressed as [1], [2], [9]

$$\begin{aligned} p(\mathbf{a},\mathbf{b},\mathbf{m}|\mathbf{y},\mathbf{q}) &= C(\mathbf{m}) \prod_{n'=1}^{n} \prod_{s=1}^{S} \prod_{k=1}^{K} h\big(\mathbf{x}_{n',k}, r_{n',k}, a_{n',k}^{(s)}, q_{n',k}^{(s)}; M_{n'}^{(s)}\big) \\ &\quad \times \prod_{m=1}^{M_{n'}^{(s)}} \Psi\big(a_{n',k}^{(s)}, b_{n',m}^{(s)}\big), \quad (4) \end{aligned}$$

where $C(\mathbf{m})$ is a normalization factor, $h\big(\mathbf{x}_{n,k}, r_{n,k}, a_{n,k}^{(s)}, q_{n,k}^{(s)}; M_n^{(s)}\big)$ is given by

$$h\big(\mathbf{x}_{n,k}, 1, a_{n,k}^{(s)}, q_{n,k}^{(s)}; M_n^{(s)}\big) = \begin{cases} \dfrac{q_{n,k}^{(s)}}{\mu^{(s)}}, & a_{n,k}^{(s)} \in \mathcal{M}_n^{(s)} \\ 1 - q_{n,k}^{(s)}, & a_{n,k}^{(s)} = 0 \end{cases}$$

$$h\big(\mathbf{x}_{n,k}, 0, a_{n,k}^{(s)}, q_{n,k}^{(s)}; M_n^{(s)}\big) = 1\big(a_{n,k}^{(s)}\big),$$

and $\Psi\big(a_{n,k}^{(s)}, b_{n,m}^{(s)}\big) \in \{0,1\}$ is an indicator function defined as

$$\Psi\big(a_{n,k}^{(s)}, b_{n,m}^{(s)}\big) \triangleq \begin{cases} 0, & a_{n,k}^{(s)} = m,\ b_{n,m}^{(s)} \neq k \\ & \quad \text{or } b_{n,m}^{(s)} = k,\ a_{n,k}^{(s)} \neq m \\ 1, & \text{otherwise.} \end{cases}$$

Note that $\Psi\big(a_{n,k}^{(s)}, b_{n,m}^{(s)}\big)$ enforces the data association constraint mentioned earlier (i.e., a target can generate at most one measurement at sensor s, and a measurement at sensor s can be generated by at most one target). The "redundant" factorization in (4) is key to obtaining an algorithm that scales well in the numbers of targets and measurements [9].

III. The Proposed Method

A. Target Detection and State Estimation

Our task is to detect the binary indicators $r_{n,k}$ in order to determine if potential target $k \in \mathcal{K}$ exists, and to estimate the states $\mathbf{x}_{n,k}$ of the detected targets, both based on the past and present measurements of all the sensors, $\mathbf{z}$. Adopting a Bayesian approach, this essentially amounts to calculating the posterior existence probabilities $p(r_{n,k}=1|\mathbf{z})$ and the posterior state pdfs $f(\mathbf{x}_{n,k}|r_{n,k}=1,\mathbf{z})$. Potential target k is then detected (considered to exist) if $p(r_{n,k}=1|\mathbf{z})$ is larger than a threshold P_{th} [14, Ch. 2], and estimates of the states $\mathbf{x}_{n,k}$ of the detected targets k are provided by the minimum mean-square error (MMSE) estimator [14, Ch. 4]

$$\hat{\mathbf{x}}_{n,k}^{\text{MMSE}} \triangleq \int \mathbf{x}_{n,k}\, f(\mathbf{x}_{n,k}|r_{n,k}=1,\mathbf{z})\, \mathrm{d}\mathbf{x}_{n,k}\,. \quad (5)$$

Here, $p(r_{n,k}=1|\mathbf{z})$ and $f(\mathbf{x}_{n,k}|r_{n,k}=1,\mathbf{z})$ can be obtained from the posterior pdf of the augmented target state, $f(\mathbf{y}_{n,k}|\mathbf{z}) = f(\mathbf{x}_{n,k}, r_{n,k}|\mathbf{z})$, according to

$$p(r_{n,k}=1|\mathbf{z}) = \int f(\mathbf{x}_{n,k}, r_{n,k}=1|\mathbf{z})\, \mathrm{d}\mathbf{x}_{n,k} \quad (6)$$

and

$$f(\mathbf{x}_{n,k}|r_{n,k}=1,\mathbf{z}) = \frac{f(\mathbf{x}_{n,k}, r_{n,k}=1|\mathbf{z})}{p(r_{n,k}=1|\mathbf{z})}\,, \quad (7)$$

respectively. The pdf $f(\mathbf{y}_{n,k}|\mathbf{z})$, in turn, can be calculated by marginalizing the joint posterior pdf $f(\mathbf{y},\mathbf{a},\mathbf{b},\mathbf{q}|\mathbf{z})$. While this is computationally infeasible, an efficient approximate marginalization can be obtained by performing BP message passing on a factor graph [15] that expresses the factorization of $f(\mathbf{y},\mathbf{a},\mathbf{b},\mathbf{q}|\mathbf{z})$.

B. Joint Posterior Distribution and Factor Graph

For the following derivation of this factor graph, we assume that the measurements $\mathbf{z}$ are observed and thus fixed, and $M_n^{(s)}$ and $\mathbf{m}$ denote the numbers of the observed measurements and the corresponding vector, respectively, i.e., they are fixed and consistent with $\mathbf{z}$. We then have

$$\begin{aligned} f(\mathbf{y},\mathbf{a},\mathbf{b},\mathbf{q}|\mathbf{z}) &= f(\mathbf{y},\mathbf{a},\mathbf{b},\mathbf{q},\mathbf{m}|\mathbf{z}) \\ &\propto f(\mathbf{z}|\mathbf{y},\mathbf{a},\mathbf{b},\mathbf{q},\mathbf{m})\, f(\mathbf{y},\mathbf{a},\mathbf{b},\mathbf{q},\mathbf{m}) \\ &= f(\mathbf{z}|\mathbf{y},\mathbf{a},\mathbf{m})\, f(\mathbf{y},\mathbf{a},\mathbf{b},\mathbf{q},\mathbf{m}) \\ &= f(\mathbf{z}|\mathbf{y},\mathbf{a},\mathbf{m})\, p(\mathbf{a},\mathbf{b},\mathbf{m}|\mathbf{y},\mathbf{q})\, f(\mathbf{y})\, p(\mathbf{q}). \end{aligned}$$

Here, we used Bayes' rule and the facts that $\mathbf{z}$ is conditionally independent of $\mathbf{q}$ given $\mathbf{a}$, that $\mathbf{a}$ implies $\mathbf{b}$, and that $\mathbf{y}$ and $\mathbf{q}$ are independent. Next, inserting (2) for $f(\mathbf{z}|\mathbf{y},\mathbf{a},\mathbf{m})$, (4) for $p(\mathbf{a},\mathbf{b},\mathbf{m}|\mathbf{y},\mathbf{q})$, (1) for $f(\mathbf{y})$, and (3) for $p(\mathbf{q})$, we obtain

$$\begin{aligned} f(\mathbf{y},\mathbf{a},\mathbf{b},\mathbf{q}|\mathbf{z}) \propto \prod_{k=1}^{K} f(\mathbf{y}_{0,k}) \left(\prod_{s=1}^{S} p\big(q_{0,k}^{(s)}\big) \right) \prod_{n'=1}^{n} f(\mathbf{y}_{n',k}|\mathbf{y}_{n'-1,k}) \\ \times \prod_{s'=1}^{S} p\big(q_{n',k}^{(s')}|q_{n'-1,k}^{(s')}\big)\, \upsilon\big(\mathbf{y}_{n',k}, a_{n',k}^{(s')}, q_{n,k}^{(s')}; \mathbf{z}_{n'}^{(s')}\big) \\ \times \prod_{m=1}^{M_{n'}^{(s')}} \Psi\big(a_{n',k}^{(s')}, b_{n',m}^{(s')}\big), \quad (8) \end{aligned}$$

with $\upsilon\big(\mathbf{y}_{n,k}, a_{n,k}^{(s)}, q_{n,k}^{(s)}; \mathbf{z}_n^{(s)}\big) \triangleq g\big(\mathbf{x}_{n,k}, r_{n,k}, a_{n,k}^{(s)}; \mathbf{z}_n^{(s)}\big) \times h\big(\mathbf{x}_{n,k}, r_{n,k}, a_{n,k}^{(s)}, q_{n,k}^{(s)}; M_n^{(s)}\big)$. The factor graph describing the factorization (8) is shown for one time step in Fig. 1.

C. BP Message Passing Algorithm

Approximations of the marginal posterior pdfs $f(\mathbf{y}_{n,k}|\mathbf{z})$—referred to as "beliefs"—can be calculated for all potential targets k in an efficient way by running iterative BP message passing [15] on the factor graph in Fig. 1. Since this factor graph contains loops, there is no unique order of calculating the messages, and different orders may result in different sets of beliefs. The order used by the proposed method is defined by the following rules: (i) Messages are not sent backward in time [16]. (ii) Iterative message passing is only performed for data association, and separately at each time step and at each

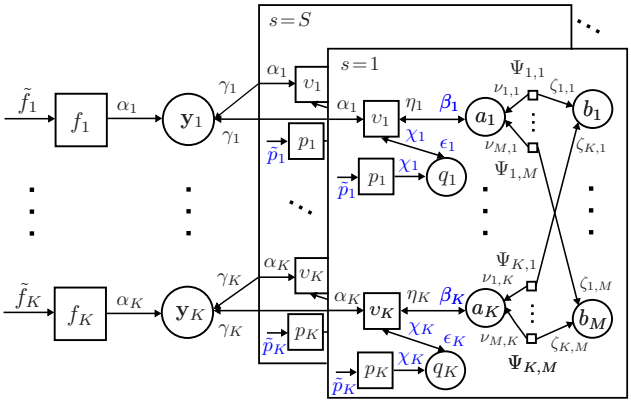

Fig. 1. Factor graph representing the factorization of $f(\mathbf{y},\mathbf{a},\mathbf{b},\mathbf{q}|\mathbf{z})$ in (8), shown for one time step. For simplicity, the time index n and sensor index s are omitted, and the following short notations are used: $f_k \triangleq f(\mathbf{y}_{n,k}|\mathbf{y}_{n-1,k})$, $p_k \triangleq p(q_{n,k}^{(s)}|q_{n-1,k}^{(s)})$, $\upsilon_k \triangleq \upsilon(\mathbf{y}_{n,k}, a_{n,k}^{(s)}, q_{n,k}^{(s)}; \mathbf{z}_n^{(s)})$, $\tilde{f}_k \triangleq \tilde{f}(\mathbf{y}_{n,k})$, $\Psi_{k,m} \triangleq \Psi(a_{n,k}^{(s)}, b_{n,m}^{(s)})$, $\alpha_k \triangleq \alpha(\mathbf{y}_{n,k})$, $\beta_k \triangleq \beta(a_{n,k}^{(s)})$, $\eta_k \triangleq \eta(a_{n,k}^{(s)})$, $\gamma_k \triangleq \gamma^{(s)}(\mathbf{y}_{n,k})$, $\chi_k \triangleq \chi(q_{n,k}^{(s)})$, $\epsilon_k \triangleq \epsilon(q_{n,k}^{(s)})$, $\nu_{m,k} \triangleq \nu_{m\to k}^{(p)}(a_{n,k}^{(s)})$, $\zeta_{k,m} \triangleq \zeta_{k\to m}^{(p)}(b_{n,m}^{(s)})$, and $\tilde{p}_k \triangleq \tilde{p}(q_{n,k}^{(s)})$. Messages that are different from, or additional to, those in [9] are depicted in blue print.

sensor. In particular, for loops involving different sensors, only a single iteration is performed.

Combining these rules with the generic BP rules for calculating messages and beliefs [15], [17], one obtains the following BP message passing operations performed at time n. First, a *prediction step* is performed for all potential targets $k \in \mathcal{K}$. This comprises the calculation of a message $\alpha(\mathbf{x}_{n,k}, r_{n,k})$ (equivalently, $\alpha(\mathbf{x}_{n,k}, 1)$ and $\alpha_{n,k}$, cf. Section II-B) as discussed in [9, Sec. III-B], and the calculation of

$$\chi\big(q_{n,k}^{(s)}\big) = \sum_{q_{n-1,k}^{(s)} \in \mathcal{Q}} p\big(q_{n,k}^{(s)}|q_{n-1,k}^{(s)}\big)\, \tilde{p}\big(q_{n-1,k}^{(s)}\big)$$

for all sensors $s \in \mathcal{S}$. Here, $\tilde{p}\big(q_{n-1,k}^{(s)}\big)$ was calculated at the previous time step $n-1$ (cf. (9) below). Next, the following steps are performed for all $k \in \mathcal{K}$ and $s \in \mathcal{S}$ in parallel:

1) *Measurement evaluation*:

$$\beta\big(a_{n,k}^{(s)}\big) = \sum_{q_{n,k}^{(s)} \in \mathcal{Q}} \int \upsilon\big(\mathbf{x}_{n,k}, 1, a_{n,k}^{(s)}, q_{n,k}^{(s)}; \mathbf{z}_n^{(s)}\big)\, \chi\big(q_{n,k}^{(s)}\big) \times \alpha(\mathbf{x}_{n,k}, 1)\, \mathrm{d}\mathbf{x}_{n,k} + 1\big(a_{n,k}^{(s)}\big)\, \alpha_{n,k}\,.$$

2) *Iterative data association* converts the messages $\beta\big(a_{n,k}^{(s)}\big)$ into messages $\eta\big(a_{n,k}^{(s)}\big)$. This step closely follows [13], [18], [19] and is identical to that in [9, Sec. III-B]; it involves iterated messages $\nu_{m\to k}^{(p)}\big(a_{n,k}^{(s)}\big)$ and $\zeta_{k\to m}^{(p)}\big(b_{n,m}^{(s)}\big)$ for $p \in \{1,\ldots,P\}$, where P is the number of iterations.

3) *Measurement update*:

$$\gamma^{(s)}(\mathbf{x}_{n,k}, 1) = \sum_{a_{n,k}^{(s)}} \sum_{q_{n,k}^{(s)} \in \mathcal{Q}} \upsilon\big(\mathbf{x}_{n,k}, 1, a_{n,k}^{(s)}, q_{n,k}^{(s)}; \mathbf{z}_n^{(s)}\big) \times \chi\big(q_{n,k}^{(s)}\big)\eta\big(a_{n,k}^{(s)}\big)\,,$$

where $\sum_{a_{n,k}^{(s)}}$ is short for $\sum_{a_{n,k}^{(s)} \in \{0,\ldots,M_n^{(s)}\}}$, and

$$\gamma_{n,k}^{(s)} = \eta\big(a_{n,k}^{(s)} = 0\big)\,.$$

4) *Detection probability update*:

$$\epsilon\big(q_{n,k}^{(s)}\big) = \sum_{a_{n,k}^{(s)}} \int \upsilon\big(\mathbf{x}_{n,k}, 1, a_{n,k}^{(s)}, q_{n,k}^{(s)}; \mathbf{z}_n^{(s)}\big)\, \eta\big(a_{n,k}^{(s)}\big) \times \alpha(\mathbf{x}_{n,k}, 1)\, \mathrm{d}\mathbf{x}_{n,k} + \eta\big(a_{n,k}^{(s)} = 0\big)\, \alpha_{n,k}$$

and

$$\tilde{p}\big(q_{n,k}^{(s)}\big) = \chi\big(q_{n,k}^{(s)}\big)\, \epsilon\big(q_{n,k}^{(s)}\big)\,. \tag{9}$$

Finally, *beliefs* $\tilde{f}(\mathbf{y}_{n,k}) = \tilde{f}(\mathbf{x}_{n,k}, r_{n,k})$ are calculated from $\alpha(\mathbf{x}_{n,k}, 1)$, $\alpha_{n,k}$, $\gamma^{(s)}(\mathbf{x}_{n,k}, 1)$, and $\gamma_{n,k}^{(s)}$ as described in [9, Sec. III-B]. These beliefs approximate the marginal posterior pdfs $f(\mathbf{y}_{n,k}|\mathbf{z}) = f(\mathbf{x}_{n,k}, r_{n,k}|\mathbf{z})$ and are used for Bayesian detection and estimation (see Section III-A) by substituting them for $f(\mathbf{x}_{n,k}, r_{n,k}|\mathbf{z})$ in (6) and (7). A particle-based implementation of the above algorithm that avoids the explicit evaluation of integrals and message products can be obtained by extending the implementation presented in [20].

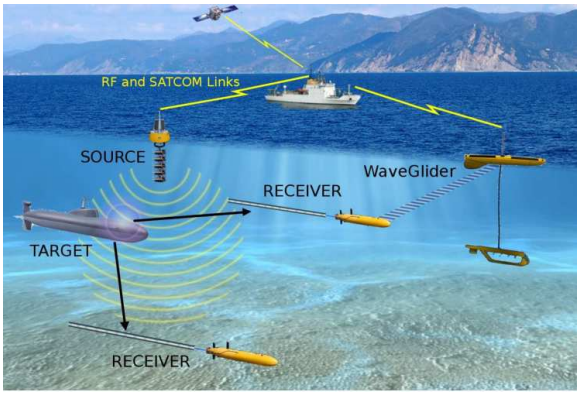

Fig. 2. Multistatic sonar network consisting of an acoustic source and two AUVs towing two receivers (hydrophone arrays). A research vessel and a wave glider act as a communication relay.

IV. Application to Multistatic Sonar Tracking

We validated the proposed method using real measurements that were collected on October 3, 2015 during the Littoral Continuous Active Sonar 2015 (LCAS15) sea trial [21].

A. Setup of Experiment and System Model

In LCAS15, a multistatic sonar network was tested for a submarine detection and tracking application. An echo repeater towed by a research vessel served as the nominal target. The measurements were provided by the network shown in Fig. 2, which consisted of an acoustic source and two receivers (sensors). The receivers were hydrophone arrays towed by two autonomous underwater vehicles (AUVs). The source operated in continuous active sonar mode, transmitting linearly frequency-modulated sweeps with a repetition period of 20s and a duty cycle of almost 100%. The receiver

signal processing computing the measurements $z_{n,m}^{(s)}$ from the output of the respective hydrophone array is described in [22]. At each sensor $s \in \{1,2\}$, due to subband processing, measurements $\mathbf{z}_n^{(s)}$ were available every 2 s. The measurements conform to a bistatic range-bearing measurement model with port-starboard ambiguity [23, Sec. II-B]. Because of the characteristics of the underwater channel and the mobility of the receivers (AUVs) and the target, the probabilities of detection are strongly time-varying.

The following assumptions and choices were used in our numerical study. The target states consist of two-dimensional (2D) position and velocity, i.e., $\mathbf{x}_{n,k} = [x_{1,n,k}\ x_{2,n,k}\ \dot{x}_{1,n,k}\ \dot{x}_{2,n,k}]^{\mathrm{T}}$. As features of the seafloor often simulate additional targets, the number of potential targets is set to $K = 8$. Target motion is modeled by the near constant velocity model $\mathbf{x}_{n,k} = \mathbf{A}\,\mathbf{x}_{n-1,k} + \mathbf{W}\mathbf{u}_{n,k}$, where $\mathbf{A} \in \mathbb{R}^{4\times 4}$ and $\mathbf{W} \in \mathbb{R}^{4\times 2}$ are chosen as in [24] and $\mathbf{u}_{n,k} \sim \mathcal{N}(\mathbf{0}, \sigma_u^2 \mathbf{I}_2)$ with $\sigma_u^2 = 0.001$ is an independent and identically distributed (iid) sequence of 2D Gaussian random vectors. The birth and survival probabilities are chosen as $p_{n,k}^{\mathrm{b}} = 0.8{\cdot}10^{-5}$ and $p_{n,k}^{\mathrm{s}} = 0.9995$, respectively. The covariance matrix of the measurement noise vectors used in the measurement model [23, Sec. II-B] is $\mathrm{diag}\{20^2, 0.0175^2\}$. The positions of the source and receivers are assumed known (since GPS position information was available). The mean number of false alarm measurements is $\mu^{(s)} = 18$. The false alarm pdf $f_{\mathrm{FA}}(\mathbf{z}_{n,m}^{(s)})$ is linearly increasing on $[0, 15000]$ m and zero outside that interval with respect to the range component, and uniform on $[0°, 360°)$ with respect to the angle component. (In Cartesian coordinates, this corresponds to a uniform distribution on a disc of radius 15000 m.) The set of detection probabilities is $\mathcal{Q} = \{0.1, 0.2, \ldots, 1\}$. The transition matrix $\mathbf{Q}^{(s)} = \mathbf{Q}$ is as follows: for $2 \le i \le 9$, $[\mathbf{Q}]_{i-1,i} = 0.05$, $[\mathbf{Q}]_{i,i} = 0.85$, and $[\mathbf{Q}]_{i+1,i} = 0.1$; furthermore, $[\mathbf{Q}]_{1,1} = 0.9$, $[\mathbf{Q}]_{1,2} = 0.1$, $[\mathbf{Q}]_{9,10} = 0.05$, $[\mathbf{Q}]_{10,10} = 0.95$, and $[\mathbf{Q}]_{i,j} = 0$ otherwise. This corresponds to the rule that with probability 0.1, the detection probability increases by 0.1, and with probability 0.05, it decreases by 0.1. (Choosing the probability of a detection probability increase higher than that of a detection probability decrease helps prevent the detection of multiple targets at the position of a single target.)

We used a particle implementation of the proposed method (cf. [20]) in which the belief $\tilde{f}(\mathbf{x}_{n,k}, r_{n,k})$ of each potential target k is represented by a set of $J = 10000$ particles and weights $\{(\mathbf{x}_{n,k}^{(j)}, w_{n,k}^{(j)})\}_{j=1}^{J}$. The sum of the weights, $p_{n,k}^{\mathrm{e}} \triangleq \sum_{j=1}^{J} w_{n,k}^{(j)}$, provides an approximation of the target existence probability $p(r_{n,k} = 1|\mathbf{z})$, and potential target k is considered to exist (is detected) if $p_{n,k}^{\mathrm{e}} > 0.75$. For each detected target k, a Monte Carlo approximation of the MMSE state estimate in (5) is then calculated as $\hat{\mathbf{x}}_{n,k} = \sum_{j=1}^{J} w_{n,k}^{(j)} \mathbf{x}_{n,k}^{(j)} / p_{n,k}^{\mathrm{e}}$. We performed $P = 20$ BP iterations for iterative data association.

B. Results

Fig. 3 shows the sensor tracks, the true target track (which was provided by GPS measurements), and the tracks estimated with the proposed method from 35 min of measurement data. After a few seconds, the target is detected and reliably tracked. There are three false tracks. The longest has a duration of roughly 15 min and is related to a feature of the seafloor. The presence of such features motivates the use of a multitarget tracking method since a single-target tracking method may track the feature instead of the target.

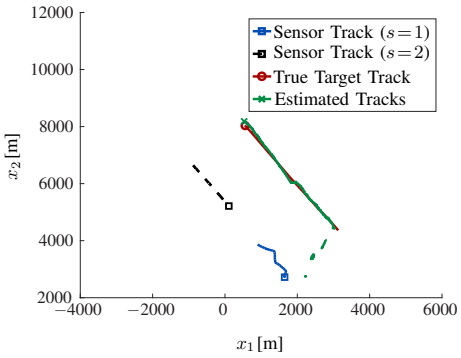

Fig. 3. Sensor tracks, true target track, and estimated tracks. The squares, circle, and cross indicate the end point of the respective trajectory.

$q_{n,k}^{(s)}$	TOT [%]	FAR [$\mathrm{s}^{-1}\mathrm{km}^{-2}$]
0.2	83	$5.1 \cdot 10^{-4}$
0.3	88	$4.9 \cdot 10^{-4}$
0.4	96	$3.4 \cdot 10^{-4}$
0.5	95	$2.6 \cdot 10^{-4}$
0.6	85	$2.1 \cdot 10^{-4}$
0.7	46	$1.3 \cdot 10^{-4}$
adaptive	95	$2.4 \cdot 10^{-4}$

TABLE I
TOT AND FAR FOR THE NONADAPTIVE METHOD WITH FIXED DETECTION PROBABILITY $q_{n,k}^{(s)}$ AND FOR THE PROPOSED ADAPTIVE METHOD.

Next, we compare the proposed adaptive method with the original nonadaptive BP method in [9]. The nonadaptive method uses identical parameters except that the detection probability $q_{n,k}^{(s)}$ is fixed for all n, k, and s. We considered six different fixed values of $q_{n,k}^{(s)}$ ranging from 0.2 to 0.7 in steps of 0.1. As performance metrics we used time-on-target (TOT) and false alarm rate (FAR) [1], [25]. TOT is the fraction of time that the target is successfully detected, where successful detection was declared if the target position estimate was within 175 m of the true target position. FAR is the normalized number of false tracks (or detections) generated in the surveillance region per unit of 2D space and time. Table I shows the TOT and FAR for both methods. For the nonadaptive method, it can be seen that large values of $q_{n,k}^{(s)}$ can significantly reduce the TOT whereas small values of $q_{n,k}^{(s)}$ result in a higher FAR. The proposed adaptive method achieves an attractive TOT–FAR tradeoff, and it does not require a manual selection of the detection probabilities (which will typically be incorrect).

Fig. 4 shows estimates of the detection probabilities $q_{n,k}^{(1)}$ and $q_{n,k}^{(2)}$ at the two sensors $s = 1$ and $s = 2$. These estimates were calculated as $\hat{q}_{n,k}^{(s)} = \sum_{i=1}^{Q} \omega_i\, \tilde{p}(q_{n,k}^{(s)} = \omega_i)$ with $\tilde{p}(q_{n,k}^{(s)})$ given by (9). It can be seen that at the beginning of the

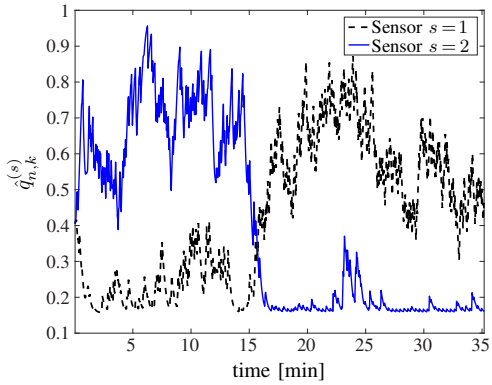

Fig. 4. Estimated detection probabilities versus time.

experiment where sensor 1 is close to the target and sensor 2 is distant from the target, $\hat{q}_{n,k}^{(1)}$ is rather high while $\hat{q}_{n,k}^{(2)}$ is low. These results are reversed after approximately 17 min, because by that time sensor 1 is distant from the target and sensor 2 is close to the target. The nonzero "floor" of $\hat{q}_{n,k}^{(s)}$ is due to the coarse discretization of $q_{n,k}^{(s)}$ defined by $\mathcal{Q}$ and the small probabilities of an increase of $q_{n,k}^{(s)}$ defined by $\mathbf{Q}$.

V. Conclusion

We proposed an adaptive extension of a belief propagation based multisensor-multitarget tracking method to the practically relevant case of unknown, time-varying detection probabilities at the individual sensors. In our approach, the detection probabilities are modeled as Markov chains and included as additional variable nodes in the factor graph. The resulting adaptive tracking method is robust to changes in the detection probabilities while retaining the low complexity and attractive scaling properties of the original nonadaptive method. The performance of the method was assessed using real data collected by a mobile underwater wireless sensor network. Our results demonstrate that the proposed adaptive method can outperform the nonadaptive method using manual tuning of the detection probabilities. The proposed approach can also be used to obtain adaptivity with respect to other model parameters.

Acknowledgments

F. Meyer, P. Braca, M. Micheli, and K. LePage are supported by the NATO Supreme Allied Command Transformation under projects SAC000601 and SAC000608. F. Hlawatsch is supported by the FWF under project P27370-N30. This work was made possible by the LCAS Multi-National Joint Research Project (MN-JRP) including as participants the NATO Centre for Maritime Research and Experimentation, the Defence Science and Technology Organisation (AUS), the Department of National Defence of Canada – Defence Research and Development Canada (CAN), the Defence Science and Technology Laboratory (GBR), Centro di Supporto e Sperimentazione Navale – Italian Navy (ITA), the Norwegian Defence Research Establishment (NOR), the Defence Technology Agency (NZL), and the Office of Naval Research (USA).

References

[1] Y. Bar-Shalom, P. K. Willett, and X. Tian, *Tracking and Data Fusion: A Handbook of Algorithms*. Storrs, CT, USA: Yaakov Bar-Shalom, 2011.

[2] R. Mahler, *Statistical Multisource-Multitarget Information Fusion*. Norwood, MA, USA: Artech House, 2007.

[3] L. Y. Pao and C. W. Frei, "A comparison of parallel and sequential implementations of a multisensor multitarget tracking algorithm," in *Proc. ACC-95*, vol. 3, Seattle, WA, USA, Jun. 1995, pp. 1683–1687.

[4] S. Deb, M. Yeddanapudi, K. Pattipati, and Y. Bar-Shalom, "A generalized S-D assignment algorithm for multisensor-multitarget state estimation," *IEEE Trans. Aerosp. Electron. Syst.*, vol. 33, no. 2, pp. 523–538, Apr. 1997.

[5] J. Vermaak, S. J. Godsill, and P. Perez, "Monte Carlo filtering for multi target tracking and data association," *IEEE Trans. Aerosp. Electron. Syst.*, vol. 41, no. 1, pp. 309–332, Jan. 2005.

[6] R. Mahler, "The multisensor PHD filter: I. General solution via multitarget calculus," in *Proc. SPIE-09*, Orlando, FL, USA, Apr. 2009.

[7] S. Nannuru, M. Coates, M. Rabbat, and S. Blouin, "General solution and approximate implementation of the multisensor multitarget CPHD filter," in *Proc. IEEE ICASSP-15*, Brisbane, Australia, Apr. 2015, pp. 4055–4059.

[8] E. Delande, E. Duflos, P. Vanheeghe, and D. Heurguier, "Multi-sensor PHD: Construction and implementation by space partitioning," in *Proc. IEEE ICASSP-11*, Prague, Czech Republic, May 2011, pp. 3632–3635.

[9] F. Meyer, P. Braca, P. Willett, and F. Hlawatsch, "Tracking an unknown number of targets using multiple sensors: A belief propagation method," in *Proc. FUSION-16*, Heidelberg, Germany, Jul. 2016, pp. 719–726.

[10] W. Blanding, P. K. Willett, Y. Bar-Shalom, and S. Coraluppi, "Multisensor track management for targets with fluctuating SNR," *IEEE Trans. Aerosp. Electron. Syst.*, vol. 45, no. 4, pp. 1275–1292, Oct. 2009.

[11] R. Mahler, B.-T. Vo, and B.-N. Vo, "CPHD filtering with unknown clutter rate and detection profile," *IEEE Trans. Signal Process.*, vol. 59, no. 8, pp. 3497–3513, Aug. 2011.

[12] G. Papa, P. Braca, S. Horn, S. Marano, V. Matta, and P. Willett, "Adaptive Bayesian tracking with unknown time-varying sensor network performance," in *Proc. IEEE ICASSP-15*, Brisbane, Australia, Apr. 2015, pp. 2534–2538.

[13] J. L. Williams and R. Lau, "Approximate evaluation of marginal association probabilities with belief propagation," *IEEE Trans. Aerosp. Electron. Syst.*, vol. 50, no. 4, pp. 2942–2959, Oct. 2014.

[14] H. V. Poor, *An Introduction to Signal Detection and Estimation*. New York, NY, USA: Springer, 1994.

[15] F. R. Kschischang, B. J. Frey, and H.-A. Loeliger, "Factor graphs and the sum-product algorithm," *IEEE Trans. Inf. Theory*, vol. 47, no. 2, pp. 498–519, Feb. 2001.

[16] H. Wymeersch, J. Lien, and M. Z. Win, "Cooperative localization in wireless networks," *Proc. IEEE*, vol. 97, no. 2, pp. 427–450, Feb. 2009.

[17] H. Wymeersch, *Iterative Receiver Design*. New York, NY, USA: Cambridge University Press, 2007.

[18] M. Chertkov, L. Kroc, F. Krzakala, M. Vergassola, and L. Zdeborová, "Inference in particle tracking experiments by passing messages between images," *PNAS*, vol. 107, no. 17, pp. 7663–7668, Apr. 2010.

[19] P. O. Vontobel, "The Bethe permanent of a nonnegative matrix," *IEEE Trans. Inf. Theory*, vol. 59, no. 3, pp. 1866–1901, Mar. 2013.

[20] F. Meyer, P. Braca, P. Willett, and F. Hlawatsch, "A scalable algorithm for tracking an unknown number of targets using multiple sensors," 2016, submitted, available online: http://arxiv.org/abs/1607.07647.

[21] A. Munafò, J. R. Bates, F. Meyer, and G. Canepa, "CAS vs. PAS performance assessment from LCAS15," Centre for Maritime Research and Experimentation (CMRE), Tech. Rep. CMRE-FR-2016-003, Jul. 2016.

[22] A. Munafò, G. Canepa, and J. R. Bates, "CAS processing results from LCAS15," Centre for Maritime Research and Experimentation (CMRE), Tech. Rep. CMRE-TPR-NU-601-03-0301-Q1, Apr. 2016.

[23] P. Braca, P. Willett, K. LePage, S. Marano, and V. Matta, "Bayesian tracking in underwater wireless sensor networks with port-starboard ambiguity," *IEEE Trans. Signal Process.*, vol. 62, no. 7, pp. 1864–1878, Apr. 2014.

[24] J. H. Kotecha and P. M. Djuric, "Gaussian particle filtering," *IEEE Trans. Signal Process.*, vol. 51, no. 10, pp. 2592–2601, Oct. 2003.

[25] S. Maresca, P. Braca, J. Horstmann, and R. Grasso, "Maritime surveillance using multiple high-frequency surface-wave radars," *IEEE Trans. Geosci. Remote Sens.*, vol. 52, no. 8, pp. 5056–5071, Aug. 2014.